

Microstructuring ceramic scaffolds for hepatocyte cell culture

S. PETRONIS¹, K.-L. ECKERT², J. GOLD¹, E. WINTERMANTEL²

¹Department of Applied Physics, Chalmers University of Technology, Gothenburg, Sweden

²Biocompatible Materials Science and Engineering, Department of Materials, ETH Zurich, Switzerland

E-mail: petronis@fy.chalmers.se

Both extracorporeal liver support devices and tissue engineering of liver for transplantation require the maintenance of functionality of liver cells (hepatocytes) in cell culture for a long time. One approach to achieve this is to optimize hepatocyte *in vitro* environment by using a scaffold with topographic structure at sub-millimeter scale which controls cell distribution. Therefore, a set of new type of titania ceramic scaffolds, containing cavities of several sizes, has been produced for deducing the best choice of cavity dimensions for culturing hepatocytes. The aim of this paper is to describe in detail the production methods and characterization of such ceramic scaffolds. Experimental production of the scaffolds consists of microfabrication of silicon templates as well as preparation and molding of titania ceramics. The templates, containing arrays of conical protrusions arranged in close-packed hexagonal order, have been achieved using microfabrication methods of photolithography and anisotropic etching in KOH at 50 °C. Protrusion dimensions and overall quality of the templates has been evaluated by scanning electron microscopy. The microfabricated templates have resulted in well-defined and reproducible cavities of corresponding dimensions on the titania ceramic surface after injection-molding. Alternatively, simple embossing of the plastified green ceramics with the silicon templates attached to a metal plate also creates cavities on the ceramic surface. While both methods yield good results, they have different advantages: the injection-molding provides a higher quality of imprints while embossing is quicker and less complicated, and is not limited by dimensions of specific molding equipment.

© 2001 Kluwer Academic Publishers

1. Introduction

Successful culturing *in vitro* of a large mass of hepatocytes (the liver parenchymal cells that perform most liver functions) is essential for both implantable and extracorporeal artificial liver systems in order to achieve sufficient metabolic replacement [1, 2]. The main challenge is to preserve differentiation and polarity of the cells, which are not automatically adopted when the hepatocytes are isolated from liver [3, 4]. Different approaches to create an optimal cell environment to preserve differentiation have been tested over the past 25 years, including a variety of substrates for cell attachment (poly(lactic acid) [5, 6], poly(lactic-co-glycolic acid) [5, 7, 8], polystyrene [9], dextran [10] polymer matrices, collagen [1, 3, 4, 7, 11–13], lactose [9], fibronectin or laminin [14] coatings and gels, alumina [15], titania [16–20] and hydroxyapatite [21] ceramics, etc.), usage of co-cultures with non-parenchymal cells [3, 8, 11, 12, 22–25] and manipulation of media composition [26–33].

In this study we have chosen the porous titania ceramic as a culture substrate since it has several

advantages over other materials for this purpose: (1) it can be made microporous, which facilitates good access and exchange of nutrients and metabolites between cells and culture media; (2) it is known as a very biocompatible implant material and its non-cytotoxicity in hepatocyte culture has been demonstrated previously [19]; (3) it induces cell aggregation without any extracellular matrix protein coatings [17, 20], and (4) it can be easily shaped by well established techniques – e.g. injection-molding. Formation of cell aggregates is favorable for the prolonged maintenance of hepatocyte differentiation, however it may also cause malnutrition and necrosis within big clusters [18]. Therefore we designed our cell culture substrates as a scaffold containing an array of conical submillimeter-size cavities, thus limiting the number of cells within them (Fig. 1). This can also be used to control spatial arrangement of hepatocytes and increase surface area for cell attachment. Preliminary studies with manually structured surfaces showed that the cells were most sensitive to the cavity size of 50–300 µm (unpublished results).

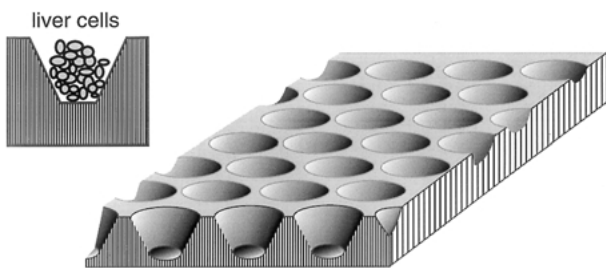


Figure 1 Schematic illustration of hepatocyte culture scaffold which should enable control over cell distribution *in vitro*.

In order to better identify an optimal cavity size, we applied microfabrication technology to obtain scaffolds with cavities of several uniform and well-defined sizes within the mentioned size range. The available methods for making precise ceramic microstructures are based on different modifications of two major ceramic shaping techniques: slip casting and injection-molding [34, 35]. The slip casting is preferred in applications where high density and homogeneity of ceramic particle distribution is important, and requires porous or lost molds for shaping [35–38]. In the case of injection-molding, normally shaped green ceramics detaches from the mold itself, so the same mold can be re-used many times. The microstructuring techniques, which we describe in this paper, are based on injection-molding and, alternatively, embossing of a thermoplastic ceramic body using microfabricated silicon templates. Templates for molding are prepared by standard photolithography and anisotropic etching of monocrystalline silicon wafers. Silicon is a good template material because photolithography can produce well controlled and defined features in the desired size range, obtaining very flat and smooth surfaces necessary for easy detachment of the template from shaped ceramics. Also, silicon has sufficient high thermal conductivity ($80\text{--}150\text{ Wm}^{-1}\text{ K}^{-1}$ at $0\text{--}100^\circ\text{C}$) and melting temperature (1410°C) required for the ceramic molding process. The main advantage of such shaping methods is that they enable the production of precise, well-defined and reproducible geometry and chemical composition of the scaffold surfaces.

2. Materials and methods

2.1. Micropatterned templates

As cavities on the ceramic surface were obtained by molding, the templates used in this process should have inverse shape, i.e. protrusions instead of cavities. The microfabrication procedure for producing them is schematically illustrated in Fig. 2(a). First, (100)-surface polished silicon wafers with an 800 nm thermal oxide layer were carefully cleaned by rinsing in acetone, isopropanol, Milli-Q[™] water, followed by oxygen plasma treatment in a reactive ion etcher (RIE, PlasmaTherm Batchtop VIII PE/RIE) in order to remove all possible organic contamination from the surface. Then the wafers were immersed into Shipley WM7213 Microposit primer for 30 sec, dried, and immediately spin-coated with 1.5 μm thick Shipley S–1813 Microposit photoresist. The coated resist was heated on a hot-plate for 1 min at 110°C to reduce residual solvent content and planarize the surface. Then the resist was exposed to UV-light

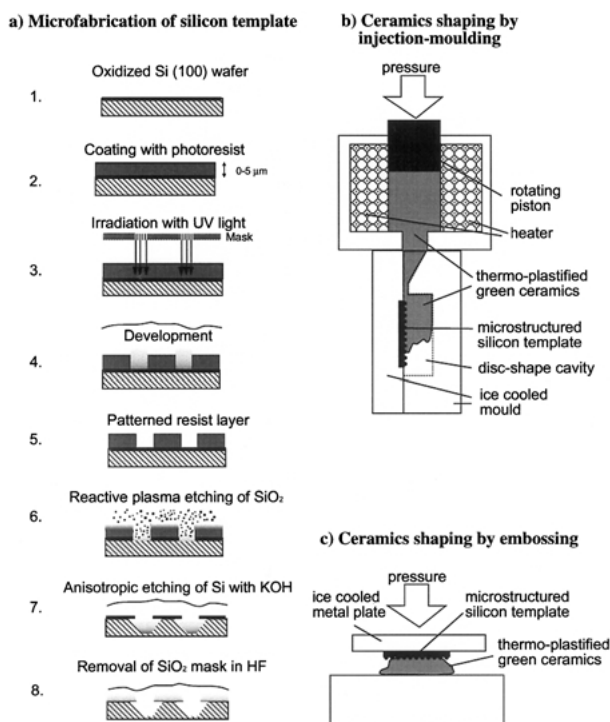


Figure 2 Microstructuring of ceramic scaffolds: (a) microfabrication procedure of silicon templates; (b) shaping of ceramics by injection-molding; (c) shaping of ceramics by embossing.

through a glass plate coated with a patterned chromium film, i.e. a photolithography mask prepared by electron beam lithography [39] (step 3 in Fig. 2(a)). The mask contained a $6 \times 6\text{ mm}^2$ transparent window patterned with $200\text{ }\mu\text{m}$ diameter non-transparent circles, arranged in hexagonal order with $100\text{ }\mu\text{m}$ edge-to-edge separation (Fig. 3). UV-exposed portions of the photoresist (i.e. area surrounding circles) were removed from the wafer surface using resist developer. The oxide layer in these areas was then etched away by CF_4/O_2 RIE (step 6 in Fig. 2(a)) while oxide under the resist remained. In such a way the pattern from the chromium mask was transferred on the oxide layer which served as an etch-resistant mask during anisotropic Si etching in potassium hydroxide (KOH) or ethylenediamine-pyrocatechol (EDP) solution. The KOH etchant consisted of 25 g potassium hydroxide

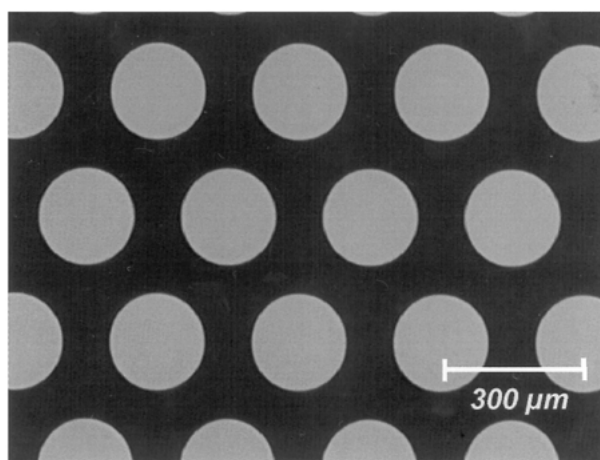


Figure 3 Micrograph of the patterned area on the photomask. Dark area is UV-transparent soda lime glass plate, bright circles are metal film circles. Diameter of the circles is $200\text{ }\mu\text{m}$, separation between them is $100\text{ }\mu\text{m}$.

in 20 ml iso-propanol and 80 ml water. EDP solution was prepared from 53 g pyrocatechol and 1 g pyrazin in 168 ml of ethylenediamine and 53 ml water. Such solutions etch in the $\langle 100 \rangle$ crystalline directions up to 100 times faster than in the $\langle 111 \rangle$ directions [40–42] resulting in formation of etched walls with a 54° inclination to the surface plane (Step 7 in Fig. 2(a)). The shapes of the etched structures were checked with surface profilometry (Tencor AlphaStep 500), interrupting the etching procedure every 10 min. When the desired etching depth was reached, the remaining SiO_2 layer was removed in 5% hydrofluoric acid (HF) solution. The final step in the microfabrication procedure of the templates was sawing the microstructured areas into $7 \times 7 \text{ mm}^2$ pieces using a diamond saw (Loadpoint MicroAce3+). The template surfaces were then characterized by scanning electron microscopy (SEM).

2.2. Ceramic injection-molding and embossing

A thermoplastic ceramic body was prepared from 20 g titania powder with $d_{50} = 9.6 \mu\text{m}$, 12 g titania powder with $d_{50} = 1.6 \mu\text{m}$, 1 g graphite powder KS6 (Lonza, Switzerland) and 3 g paraffin (MP 64°C , Fluka, Switzerland). After thorough mixing in the warm state, a plastic body was obtained. Shaping was performed using a laboratory injection-molding unit (MiniMax-Molder, Atlas SFTS) operated at 125°C (Fig. 2(b)) or by embossing the pre-cooled mold (0°C) into the hot (125°C) plastic body (Fig. 2(c)). For injection-molding a special metallic injection mold for ceramic discs, 10.5 mm in diameter and 1.5 mm deep, was fabricated (Fig. 2(b)). A depression was spark-eroded into the mold to accommodate the micropatterned silicon templates as precisely as possible. The structured templates were glued into the depression using low-viscosity cyan acrylate glue. Alternatively, the silicon templates were fixed in the same way to a flat metal plate for ceramics shaping by embossing (Fig. 2(c)).

After shaping the green ceramic parts were pyrolyzed by heating to 300°C at a rate of 7.5°C per hour, then sintered at 1350°C for 25 min. Obtained ceramic samples were characterized using SEM and confocal laser microscopy (CLSM).

3. Results and discussion

3.1. Investigation of anisotropic etching of silicon for microstructuring templates

The SEM studies of the micropatterned silicon wafers after etching in KOH are presented in Fig. 4. The templates contain arrays of conical protrusions arranged in close-packed hexagonal order, thus maximizing the density of the pits at the ceramic surface. Protrusion diameters range between $230\text{--}300 \mu\text{m}$ at the base of the cones and $20\text{--}150 \mu\text{m}$ at the truncated top, depending on protrusion heights, which are $50\text{--}135 \mu\text{m}$. It can be seen that the entire etched surface is smooth. This is very important for the easiest release of the shaped ceramics from the template. However, in some cases several micropyramids ($< 10 \mu\text{m}$ height) appeared on the bottom surface around the base of the cones when the

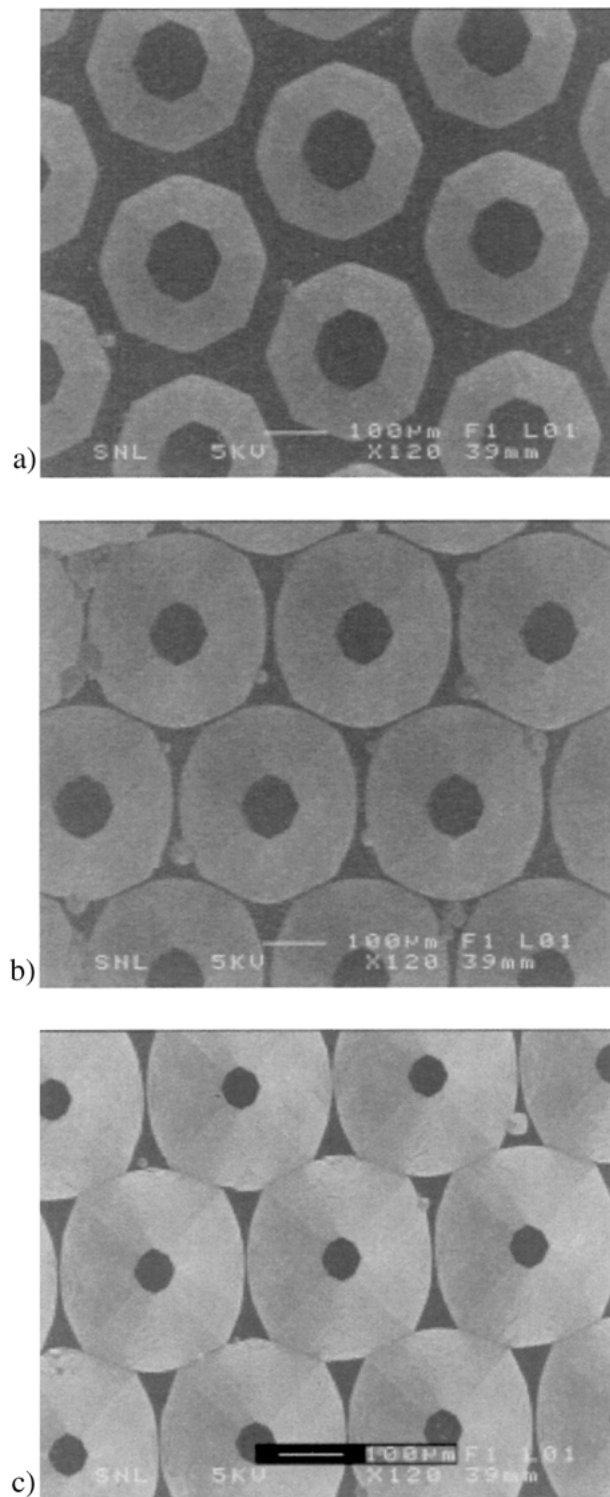


Figure 4 SEM images (top-view) of the microfabricated silicon templates, made using a photomask with $130 \mu\text{m}$ diameter circles. Etching was performed in KOH solution at 80°C . By varying etching time, different protrusion heights were achieved: (a) $73 \mu\text{m}$, (b) $103 \mu\text{m}$, (c) $130 \mu\text{m}$.

etching temperature was $70\text{--}90^\circ\text{C}$ (Fig. 5(a)). The origin of pyramid formation during etching is not completely clear at present, although it is known that purity [43] and type [41] of the etchant, etching conditions [41], and surface inhomogeneities [44] are the main determining factors for this phenomenon. Therefore we tried to use EDP etchant instead of the KOH to avoid formation of such micropyramids, as has been demonstrated by Kern [41]. However, it appeared that EDP etches more anisotropically the $\{111\}$ and $\{211\}$ planes than

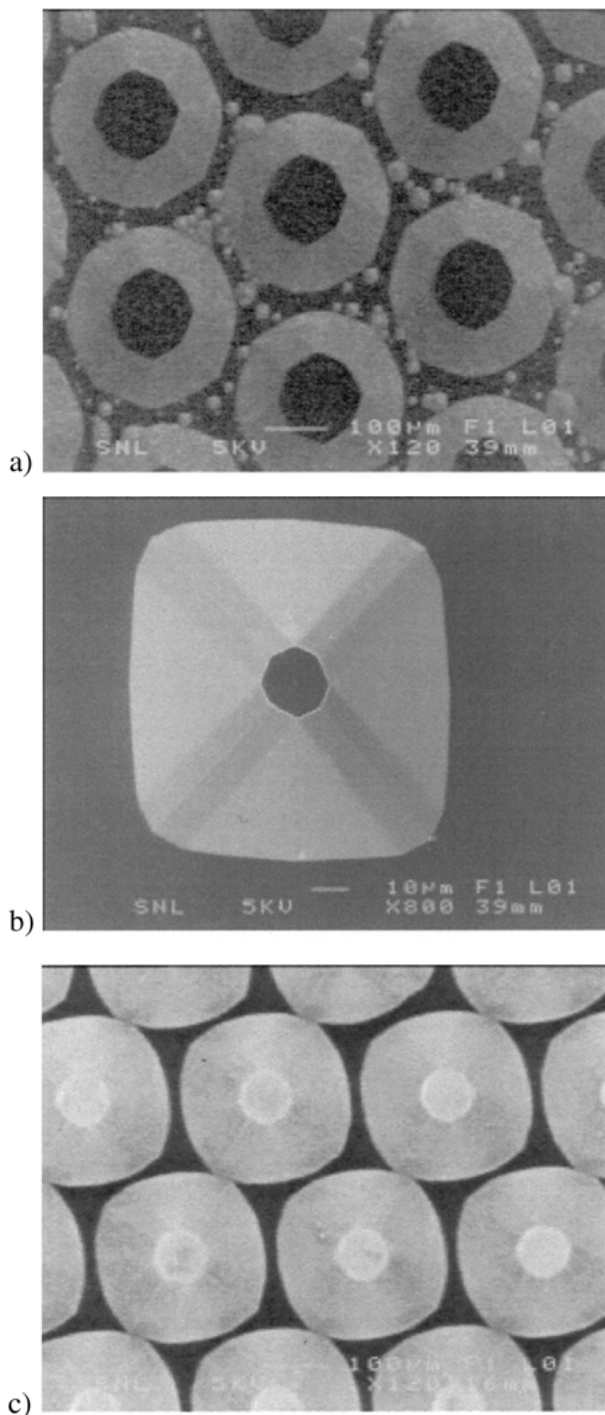


Figure 5 SEM images (top-view) of templates made by anisotropic etching under different conditions: (a) in KOH at $\approx 80^\circ\text{C}$; many micropyramids can be seen around $70\ \mu\text{m}$ height protrusions; (b) in EDP at 112°C ; no micropyramids, however protrusions are only $42\ \mu\text{m}$ height and have already lost their round shape; (c) in KOH at 50°C ; protrusions are $120\ \mu\text{m}$ height and still round; no micropyramids are formed.

KOH, so protrusions lose their round shape and adopt a faceted shape, as can be seen by comparing SEM pictures in Fig. 5(b) and Fig. 5(c). This is not a desirable effect because sharp edges of faceted protrusions contribute to an interlocking of the shaped sample and the template, causing more difficult mold release. Therefore, additional studies on etching with KOH have been performed. Consequently, it was discovered that formation of the micropyramids is hindered and protrusions still have a round shape if the etching is done at 50°C which is a temperature much lower than recommended in the

literature ($\approx 80^\circ\text{C}$) (Fig. 5(c)). This supports the hypothesis that a cause of micropyramid appearance is formation of hydrogen bubbles by the etching reaction which temporarily mask the surface [44]. At lowered temperature the etching rate is decreased significantly, therefore the time period, when the bubbles mask the surface, is too short to result in a significant defect. Etching at higher temperatures (to increase etching rate) combined with ultrasonification (to improve hydrogen bubble detachment from the surface), as recommended by Baum and Schiffrin [44], was not effective in our case – micropyramidal hillocks were densely covering etched surfaces.

3.2. Molding and evaluation of ceramic scaffolds

In initial trials of injection-molding of the ceramics, mold release after injection of the ceramic body was not achieved. This led to frequent damage of the brittle silicon templates. Improvement of the glueing technique for optimized mechanical and thermal contact with the rest of the mold prevented chip fracture and reduced damage of the structured surface. Mold cooling in ice water prior to shaping facilitated release of the green body ceramics too. The shaped samples could be released from the mold without applying any external mechanical force. It is possible that this improvement of mold release was achieved not only because of decreased temperature of the mold, but also due to a thin layer of water which condensed from room air during cooling, and worked as a release agent. Pre-cooling of a metal plate holding silicon template was necessary when shaping ceramics by embossing, too.

After sintering, the surface of the ceramic samples produced by both methods reflected very well the shape of the silicon inlays (Fig. 6), which indicated good flow properties of the ceramic body. The porosity of the fired ceramics is about 25% as measured previously [17, 20]. No significant distortion of the intended surface topography due to ceramic processing was observed. Small damages at the surface are caused by local adhesion between the template and green body ceramics during demolding or embossing plate release. This leads to residues of ceramic body on the template which have to be removed at regular intervals by dissolution in tetrahydrofuran (THF) in order to reuse the template.

The molded cavities are uniform, with thin rims between them which minimize space for hepatocyte attachment outside the cavities. The rims and edges at the bottom of cavities appear sharper in the injection-molded sample compared to the embossed one. Also, CLSM studies (Fig. 7) revealed that the cavities in injection-molded ceramics are about 2% deeper (e.g. template with $103\ \mu\text{m}$ height protrusions yielded ceramic scaffolds with $R_z = 102\ \mu\text{m}$ when using injection-molding, and $R_z = 101\ \mu\text{m}$ when using embossing), indicating that the template geometry is reproduced better by injection-molding technique, although this difference is not significant for our application. On the other hand, the embossing was performed using simple equipment, was quicker, and gave fewer problems with template release. An additional advantage of the embossing technique was

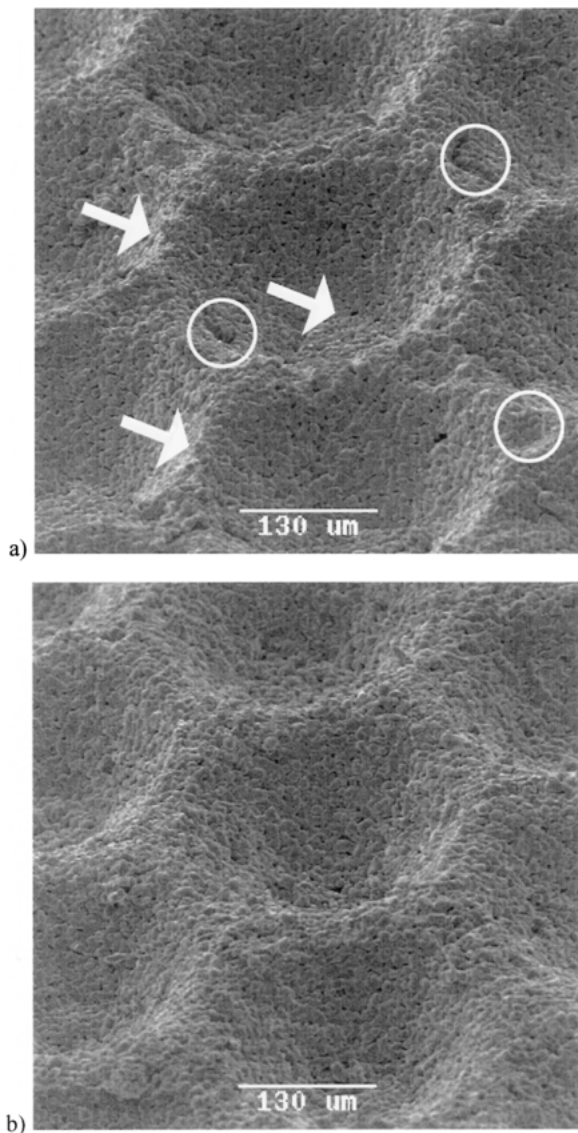


Figure 6 SEM images of (a) injection-molded and (b) embossed scaffolds using a template with 103 μm height protrusions. Arrows indicate the small details that were better reproduced by the injection-molding than by the embossing method. Circles surround small irregularities of the surface created by local adhesion between the template and green ceramics during demolding.

that the patterned area was not limited by the dimensions of the injection-molding equipment. Therefore we believe that the embossing technique of ceramics shaping has a potential for large scale micropatterning applications.

This study confirms that combination of photolithography, anisotropic etching and injection-molding or embossing is a promising way to make ceramic scaffolds for tissue engineering as well as for other applications where well-defined and reproducible surfaces at small scale are needed.

The prepared set of scaffolds will be further used in hepatocyte culture for deducing the best choice of cavity size. These experiments will be presented in another report. Preliminary 24 h cell culture studies of rat liver hepatocytes on the ceramics with 102 μm depth cavities (Fig. 8) show that the cells mainly aggregate within the cavities, and only single cells or small clusters are

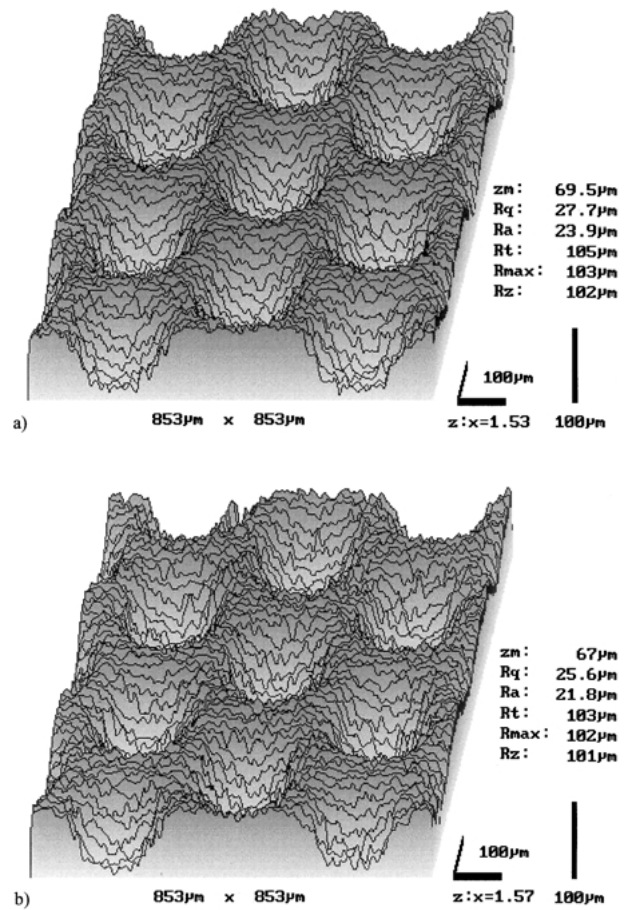


Figure 7 CLSM profile images and surface topography parameters of (a) injection-molded and (b) embossed scaffolds using a template with 103 μm height protrusions. The topographical values of embossed samples are slightly reduced compared to the values of injection-molded samples (see text).

attached to the rims between the pits, i.e. hepatocyte distribution is actually affected by the surface topography.

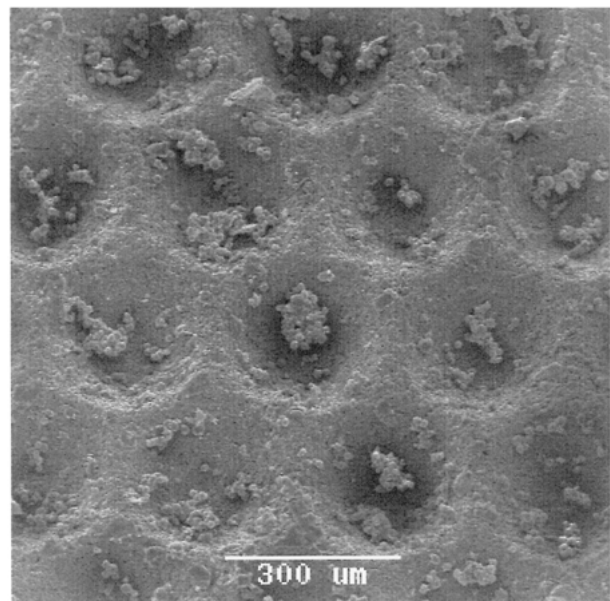


Figure 8 Rat liver hepatocytes cultured on the ceramics with 102 μm depth cavities for 24 h (preliminary study). The cells mainly aggregate within the cavities, and only single cells or small clusters are attached to the rims between the pits.

4. Conclusions

A new type of titania ceramic scaffold for controlling hepatocyte distribution in cell culture is suggested. Its well-defined surface morphology (array of sub-millimeter cavities) can be created by molding thermoplastified ceramics using microfabricated silicon templates. Microfabrication of the silicon templates is based on photolithography and anisotropic wet etching of silicon. Formation of micropyramidal hillocks should be considered if KOH is used as the anisotropic etchant, in order to assure uniformity of the cavities and the rims between them on the molded scaffold. Optimization of etching temperature is a promising route to prevent this drawback of the etching method.

Both injection-molding and embossing can be used successfully for shaping of titania ceramics if mold or embossing plate is cooled in ice-water to facilitate release of shaped ceramics from the template. However, the injection-molding gives better reproducibility of small details of the template, while the embossing method has the benefits of simplicity and expandability for large area micropatterning.

Acknowledgments

Parts of this research have been funded by the Swedish Foundation for Strategic Research (SSF), by the Swedish Biomaterials Consortium, and by a University grant from ETH, Zurich. Microfabrication and characterization of the silicon templates have been performed using facilities of the Swedish Nanometer Laboratory, Chalmers University of Technology.

References

1. R. LANGER and J. P. VACANTI, *Science* **260** (1993) 920.
2. M. W. DAVIS and J. P. VACANTI, *Biomaterials* **17** (1996) 365.
3. P. BALL, *Nature* **391** (1998) 128.
4. P. V. MOGHE, F. BERTHIAUME, R. M. EZZELL, M. TONER, R. G. TOMPKINS and M. L. YARMUSH, *Biomaterials* **17** (1996) 373.
5. E. KARAMUK, J. MAYER, B. EDER, S. RITTER, E. WINTERMANTEL and T. AKAIKE, in Abstracts of the 1st International Conference on Biomaterials BIOSURF-I, Zürich, September 1997, (ETHZ, Zürich, 1997) p. P26.
6. D. J. MOONEY, K. SANO, P. M. KAUFMANN, K. MAJAHOD, B. SCHLOO, J. P. VACANTI and R. LANGER, *J. Biomed. Mater. Res.* **37** (1997) 413.
7. C. S. RANUCCI, F. C. KAUFFMAN and P. V. MOGHE, in Transactions of the 24th Annual Meeting of the Society for Biomaterials, vol. XXI, San Diego, April 1998, edited by B. Goodman, (Society for Biomaterials, San Diego, 1998) p. 81.
8. M. J. POWERS, C. A. SUNDBACK, S. S. KIM, H. UTSUNOMIYA, M. S. BENVENUTO, B. M. WU, M. J. CIMA, J. P. VACANTI and L. G. GRIFFITH, in Abstracts of the 1st Smith & Nephew International Symposium, "Advances in Tissue Engineering and Biomaterials", York, July 1997, edited by A. Sugget, (York, 1997) p. S3.
9. A. T. GUTSCHE, H. LO, J. ZURLO, J. YAGER and K. W. LEONG, *Biomaterials* **17** (1996) 387.
10. J. ROZGA, E. MORSIANI, E. LEPAGE, A. D. MOSCIONI, T. GIORGIO and A. A. DEMETRIOU, *Biotechnol. Bioeng.* **43** (1994) 645.
11. Y. KONO, S. YANG and E. A. ROBERTS, *In Vitro Cell Dev. Biol. Anim.* **33** (1997) 467.
12. S. N. BHATIA, M. L. YARMUSH and M. TONER, *J. Biomed. Mater. Res.* **34** (1997) 189.
13. E. KNOP, A. BADER, K. BOKER, R. PICHLMAYR and K. F. SEWING, *Anat. Rec.* **242** (1995) 337.
14. P. R. SUDHAKARAN, S. C. STAMATOGLU and R. C. HUGHES, *Exp. Cell Res.* **167** (1986) 505.

15. E. WINTERMANTEL, J. MAYER, J. BLUM, K.-L. ECKERT and P. LÜSCHER, *Biomaterials* **17** (1996) 83.
16. K.-L. ECKERT, S.-W. HA, M. MATHEY and E. WINTERMANTEL, *Bioceramics* **8** (1995) 447.
17. K.-L. ECKERT, B. STIEGER, M. PETITMERMET, S.-W. HA, A. BRUININK, F. BIRCHLER, M. GERSBACH-FEY, P. MEIER-ABT and E. WINTERMANTEL, in Abstracts of the 13th European Conference on Biomaterials, Göteborg, September 1997, edited by P. Thomsen, (ESB, Göteborg, 1997) p. P90.
18. K.-L. ECKERT, S. PETRONIS, B. STIEGER, P. MEIER-ABT, J. GOLD and E. WINTERMANTEL, in Abstracts of the 2nd International Conference on Biomaterials BIOSURF-II, Lausanne, October 1998, edited by M. Hofmann, G. Schmid, J.A. Hubbell, M. Textor and H. Hofmann (Repro EPFL, Lausanne, 1998) p. B19.
19. J. BLUM, K.-L. ECKERT, A. SCHROEDER, M. PETITMERMET, S.-W. HA and E. WINTERMANTEL, *Bioceramics* **9** (1996) 89.
20. K.-L. ECKERT, B. STIEGER, R. GADOW, P. J. MEIER and E. WINTERMANTEL, in Proceedings of the 23rd Annual Cocoa Beach Conference and Exposition on Composites, Advanced Ceramics, Materials and Structures, Cocoa Beach, January 1999, (in press).
21. T. SUZUKI, *Nippon Rinsho* **55** (1997) 2140.
22. S. N. BHATIA, U. J. BALIS, M. L. YARMUSH and M. TONER, *Biotechnol. Prog.* **14** (1998) 378.
23. M. A. TALAMINI, M. P. MCCLUSKEY, T. G. BUCHMAN and A. DE MAIO, *Am. J. Physiol.* **275** (1998) R203.
24. M. K. AUTH, M. OKAMOTO, Y. ISHIDA, A. KEOGH, S. H. AUTH, J. GERLACH, A. ENCKE, P. MCMASTER and A. J. STRAIN, *Transpl. Int.* **11** (1998) S439.
25. M. KOIKE, M. MATSUSHITA, K. TAGUCHI and J. UCHINO, *Artif. Organs* **20** (1996) 186.
26. A. M. BARRECA, A. VOCI, P. D. LEE, M. ARVIGO, V. GHIGLIOTTI, E. FUGASSA, G. GIORDANO and F. MINUTO, *Eur. J. Endocrinol.* **137** (1997) 193.
27. D. C. HOOPER, C. J. STEER, C. A. DINARELLO and A. C. PEACOCK, *Biochim. Biophys. Acta* **653** (1981) 118.
28. T. A. KOCAREK, E. G. SCHUETZ and P. S. GUZELIAN, *In Vitro Cell Dev. Biol.* **29A** (1993) 62.
29. Y. LI, G. L. SATTLER and H. C. PITOT, *In Vitro Cell Dev. Biol. Anim.* **31** (1995) 867.
30. G. A. VAN'T KLOOSTER, F. M. WOUTERSEN-VAN NINANTEN, W. R. KLEIN, B. J. BLAAUBOER, J. NOORDHOEK and A. S. VAN MIERT, *Xenobiotica* **22** (1992) 523.
31. Y. VANDENBERGHE, D. RATANASAVANH, D. GLAISE and A. GUILLOUZO, *In Vitro Cell Dev. Biol.* **24** (1988) 281.
32. P. WATTS, M. D. SMITH, I. EDWARDS, V. ZAMMIT, V. BROWN and H. GRANT, *J. Hepatol.* **23** (1995) 605.
33. J. Z. TONG, O. BERNARD and F. ALVAREZ, *Exp. Cell Res.* **189** (1990) 87.
34. V. PIOTTER, T. HANEMANN, R. RUPRECHT and J. HAUSSELT, *Microsys. Techn.* **3** (1997) 129.
35. W. BAUER, H. RITZHAUPT-KLEISSL and J. HAUSSELT, *Microsys. Techn.* **4** (1998) 125.
36. R. KNITTER, E. GÜNTHER, C. ODEMER and U. MACIEJEWSKI, *Microsys. Techn.* **2** (1996) 135.
37. W. BAUER, H. RITZHAUPT-KLEISSL and J. HAUSSELT, *Ceramics International* **25** (1999) 201.
38. H. RITZHAUPT-KLEISSL, W. BAUER, E. GÜNTHER, J. LAUBERSHEIMER and J. HAUSSELT, *Microsys. Techn.* **2** (1996) 130.
39. B. NILSSON, "Mask making – a short guide", (Chalmers University of Technology, 1996).
40. D. B. LEE, *J. Appl. Phys.* **40** (1969).
41. W. KERN, *RCA Review* **39** (1978) 278.
42. H. SEIDEL, L. CSEPREGI, HEUBERGER and H. BAUMGÄRTEL, *J. Electrochem. Soc.* **137** (1990) 3612.
43. T. A. KWA and R. F. WOLFFENBUTTEL, *J. Micromech. Microeng.* **5** (1995) 95.
44. T. BAUM and D. J. SCHIFFRIN, *ibid.* **7** (1997) 338.

Received 4 January
and accepted 24 January 2000